A methodology to estimate mechanical losses and its distribution during a real driving cycle

Bernardo Tormos[a], Jaime Martín[a], Benjamín Pla[a], Antonio J. Jiménez-Reyes[a,*]

[a]*Instituto Universitario CMT - Motores Térmicos, Universitat Politècnica de València, 46022, Valencia, Spain*

Abstract

Reducing mechanical losses in internal combustion engines has been a recurrent research topic over the past few decades. Despite mechanical losses are a key issue that should be carefully addressed to reduce fuel consumption and emissions, its distribution amongst engine elements is barely covered in literature. Recent work has shown the potential advantage of using low viscosity engine oils to reduce fuel consumption, however, there is reduced knowledge on mechanical losses distribution under transient conditions. In this work, a model is presented that predicts not only the total friction losses of an engine, but determines the amount of friction energy lost in piston-ring assembly, engine bearings, camshaft and engine auxiliaries in driving cycles representing a real driving route. The final results of the simulation predicts, with 2% error, fuel consumption, energy expended by the driven wheel and mechanical losses of the engine. This methodology reduces the computational cost to estimate key engine parameters in a real driving cycle such as: mechanical losses and its distribution, fuel consumption... as the total calculation time is 10 seconds per cycle simulated.

Keywords: Driving cycles; friction model; mechanical losses distribution; Numerical analysis

*Corresponding author
Email address: anjire1@mot.upv.es (Antonio J. Jiménez-Reyes)

1. Introduction

The transport sector is a contributor to climate change, accounting about 22% of the energy related world GHG emissions [1]. Furthermore, the transport sector is a large consumer of fossil fuels, as well as other types of fuel [2], [3]. In a typical passenger car, 21% of the energy introduced into the engine is used to move the vehicle and the remaining 79% is released to the ambient[4]. Around 17% of that lost energy is dissipated to move mechanical elements with relative movement to each other. European regulations are becoming more demanding with pollutant emissions from light-duty vehicles to reduce the impact on climate change [5], thus CO_2 emissions, main issue for greenhouse effect, has been set to 95 g/km in 2020 for the average fleet on each car manufacturer [6].

The fuel consumption of a vehicle depends, mainly, on the base engine. Several strategies have been taken in account along this field:

- The downsizing philosophy, which consists of reducing the total displacement engine for a given vehicle mass and in coupling the engine to a turbocharger [7],[8].
- Improve thermodynamic engine cycle performance by means of improving combustion efficiency [9], [10].
- Reduce engine friction by means of surface texturing and coating [11], [12].
- Modify the viscosity of the engine lubricant and oil composition [13],[14].

And also, other external factors that can influence the fuel consumption: driving mode, traffic [15], [16], [17] and optimal gear-shifting strategy [18].

One way to estimate the polluting emissions and fuel consumption of a vehicle is by simulating real driving cycles. Authors in [19] simulate a cycle developed in a city to compare the consumption of various vehicles. Also, in [20] the use of GT-Drive software is proposed to model driving cycles to estimate fuel consumption and polluting.

The current challenge is to reduce the fuel consumption of vehicles in order to comply with current and oncoming regulations. One potential strategy, with

a proven cost-effective way to increase engine efficiency and decrease engine emissions, is the reduction of the viscosity of engine lubricating oils in order to reduce mechanical losses [21], [22], [23], [24]. In the aforementioned publications, experimental studies were carried out during driving cycles to estimate the fuel savings produced by different lubricating oils. While these works were mainly experimental, a simulation tool is currently interesting to perform an optimal study of engine performance in a real driving cycle against different lubricating oils.

In this work a model to estimate the lost friction energy of each element contributing to mechanical losses during a driving cycle measured has been developed. To do this, in a previous work [25] a model that is able to predict the energy consumed in the elements with relative movement was developed. In this work, the model has been adjusted to accurately predict the vehicle performance under real operating conditions. In this way, it has been possible to estimate the friction energy dissipated in each engine component: the piston-ring assembly, camshaft, engine bearing and auxiliaries assembly.

2. Experimental tools

In this section, the experimental tools will be described. In this work, both stationary and transients experiments were realized. The stationary test were carried out in order to obtain the key parameters necessary to simulate and calculate the mechanical losses and its distribution in the engine under different conditions of load and engine speed. After that, the transients test were realized in a transient test bench described below.

2.1. Stationary engine test bench

The engine operation maps (fuel consumption, mechanical losses versus engine speed and brake torque) have been obtained in a stationary test bench shown in Figure 1. Those data will be inputs in the simulation software. The engine, whose main characteristics are presented in Table 1, is instrumented

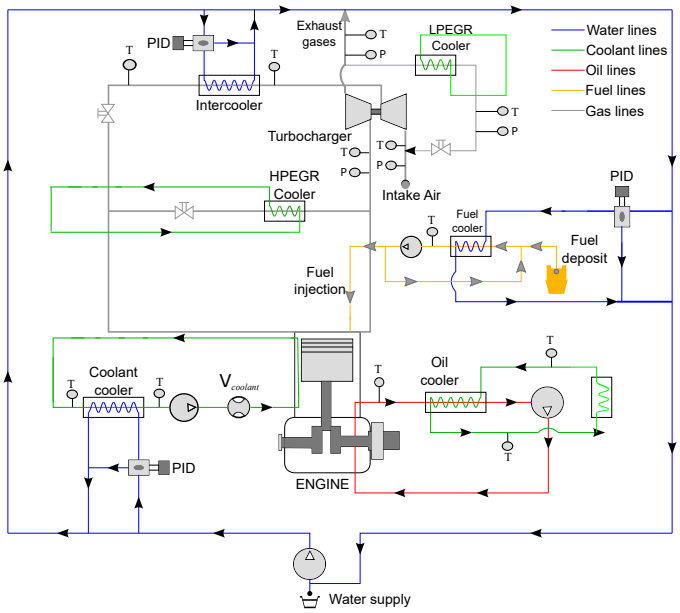

Figure 1: Engine Test Bench Scheme

with 4 AVL GH13P piezo-electric transducers installed at the glow plug hole of each cylinder to measure the in-cylinder pressure. A Kistler 2011B amplifier is used for conditioning the signal adquired by the piezo-electric transducers which was calibrated according to [26].

K-type thermocouples have been installed to measure mean temperatures of the intake and exhaust gases, coolant and lubricant. The injected fuel was measured with an AVL 733S fuel meter, the air flow with a DN80 sensyflow, the blow-by leakage, key variable to obtain the engine piston assembly friction, was measured with an AVL blow-by-meter.

The acquisition and control of the low frequency signals was performed with STARS. The instantaneous in-cylinder pressure signals were acquired by means of a Yokogawa DL708E Oscillographic recorder with 16 A/D converter module.

Finally, in order to acquire the engine registered by the engine control unit (ECU), the ETAS INCA software was used.

2.2. Vehicle transient test bench

While an stationary engine test bench has been used to obtain the required experimental information for the model calibration and experimental maps, the evaluation of the mechanical losses distribution during real driving conditions has been carried out in a complete vehicle equipped with the engine under study. The main specifications of the vehicle are shown in Table 1. The powertrain has been instrumented with a subset of sensors used in the engine test bench: pressure and temperature sensors at different parts of the air loop system as well as air mass flow and pollutant concentrations. A rapid prototyping dSpace system is used in order to manage all the fuel, emissions and performance measurements from different sensors and acquisition systems. In particular, the setup gathers information from both the standard vehicle sensors, accessing the ECU variables in real time through ETK port, and the research instrumentation by means of additional CAN channels. The vehicle is installed in a dynamic vehicle test bench equipped with variable frequency fast response dynamometers at the hubs of the driving wheels (Rototest Energy 260 2WD). In this way, the torque and speed at the driving wheels is measured. This system simulates on-road conditions considering vehicle and powertrain inertia and the resistance caused by aerodynamic drag, tyre rolling and road gradient. In this sense, different driving cycles registered in real driving conditions (defined by a sequence of vehicle speeds and road gradients) can be reproduced in a laboratory under controlled conditions with additional sensors and peripherals. The chosen route is a 33 km daily commute between two cities in Spain, consisting of urban sections, highway driving and rural roads. The urban section corresponds to the first 180 seconds of the cycle. Then, in the second section of the cycle and the most durable corresponds to the highway. Finally, the cycle ends with a rural road. This route has been tested with three different driver profiles, simulating standard operating conditions. The speed profile for each driving condition is shown in Figure 2. In addition to the speed profile, the altitude of the route is also considered and represented. The route present a positive height difference of 289 meters.

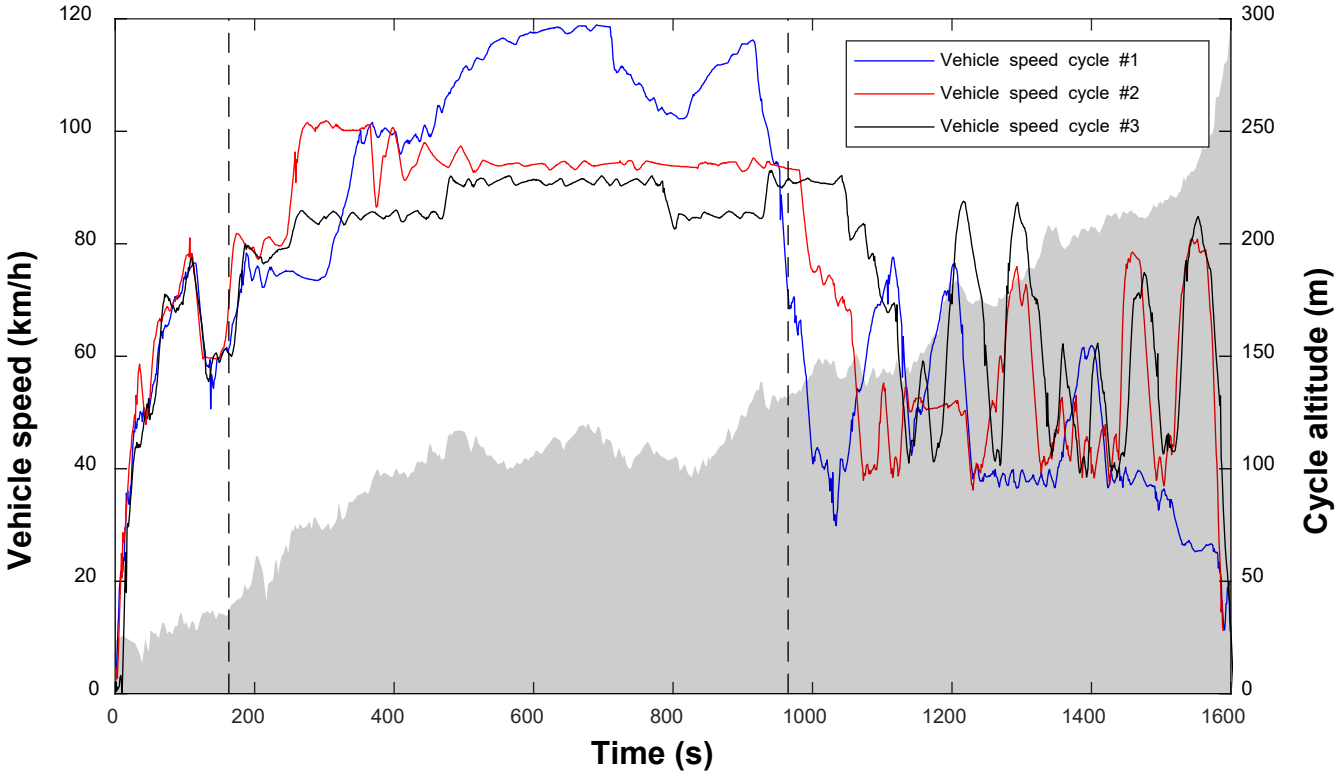

Figure 2: Speed profiles

Table 1: Tested vehicle specifications

Feature	Description	Feture	Description	Feature	Description	Feature	Description
Mass [kg]	1580	Displacament [cm^3]	1598	Tire diameter [mm]	700	Gear Ratio 4th [-]	0.947
Drag Coefficient [-]	0.35	Max power [kW]	96 @ 4000 rpm	Vehicle Wheelbase [m]	2.705	Gear Ratio 5th [-]	0.723
Frontal area [m^2]	2.2	Max Torque [Nm]	320 @ 1750 rpm	Gear Ratio 1st [-]	3.727	Gear Ratio 6th [-]	0.596
Friction coefficient [-]	0.01	Breathing method	turbocharger, intercooler, VGT	Gear Ratio 2nd [-]	2.043	Final Drive Ratio [-]	4.428
Engine Type	Euro 6, inline-four, CI	Emissions control	HP-EGR, LP-EGR, DOC, DPF, LNT	Gear Ratio 3rd [-]	1.322	Transmission Efficiency [-]	0.9

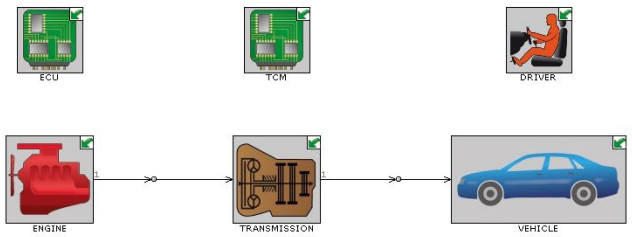

Figure 3: GT Power model scheme

3. Simulation tool and model description

This section explain the simulation tool used in this work and a brief description about the theoretical model implemented in order to solve the equations which predicts the engine and vehicle performance during the different driving cycles.

3.1. GT-Drive

Real driving cycles have been simulated in GT-Drive+, a well known simulation software developed by Gamma Technologies which predicts the vehicle performance during the cycle and it provides the necessary key parameters that it can not be measured during the transients test. Several authors have used the 1D software GT-Suite in order to predict the engine emission and fuel consumption in a real driving emission (RDE) tests [27], [28], [20], [29]. In Figure 3 a graph representation of the model is presented. On it, the different units which make up the complete model can be seen, such as: engine, where the stationary engine maps are included, driver where the cycle speed is the main input, etc.

3.2. Model description

The model has been defined to predict the engine performance during a real driving cycle by means of an engine map defined in stationary conditions. The differential equations of motion for the driveline components and the vehicle, equation 1, is used to calculate instantaneous speeds and torque in the system. The BMEP, IMEP and fuel consumption maps have been measured under

stationary conditions in a test bench as a function of load and engine speed. FMEP has been calculated by means of net IMEP method described in [25]. The previous maps have been used to calculate the fueling rate and instantaneous mechanical losses in transients condition, interpolating the instantaneous engine torque and engine speed required in the driving cycle. Finally, the model calculates the engine speed and torque required during the driving cycle as a consequence of vehicle characteristics and speed.

$$\begin{aligned}\tau_{drv,v} = &\left[I_{trans,1} + \frac{I_{trans,2}}{R_t^2} + \frac{I_{axl}}{R_d^2 R_t^2} + \frac{M_{veh} r_{whl}^2}{R_d^2 R_t^2}\right] \frac{d\omega_{drv}}{dt} \\ &- \left[\frac{I_{trans,2}}{R_t^3} + \frac{I_{dsh}}{R_t^3} + \frac{I_{axl}}{R_d^2 R_t^3} + \frac{M_{veh} r_{whl}^2}{R_d^2 R_t^3}\right] \omega_{drv} \frac{dR_t}{dt} \\ &+ \left[\frac{F_{aer} + F_{rol} + F_{grd}}{R_d R_t}\right] r_{whl}\end{aligned} \tag{1}$$

The first term of the equation shows the necessary torque to accelerate the effective inertia of the entire drivetrain. The terms $I_{trans,1}$ and $I_{trans,2}$ quantify the input and output Transmission Moment of Inertia respectively. I_{dsh} and I_{axl} are driveshaft and axle moment of inertia the wheels' moment of inertia are included in the last term described. R_d and R_t represent the transmission gear ratio and final drive ratio of the vehicle. M_{veh} is the vehicle mass and ω_{drv} indicates the instantaneous vehicle speed in fuction of the time (s) related of the wheel radius r_{whl}. The second term is an additional term derived from the effective inertia equation due to the gear ratio may be transient, so, it represents the load induced by a transient gear ratio. Finally, the third term represents the external forces such as: aerodynamic forces (F_{aer}), rolling resistance force (F_{rol}) and gravity force (F_{grd}).

4. Results and discussion

This section compares the results obtained in the experimental driving cycle test against those obtained in the developed model. To validate the engine model, the fuel consumption during the cycles studied has been compared. To

validate the powertrain model, a comparison has been made with the accumulated energy expended in driven wheels and the engine speed at each moment of the cycle.

4.1. Model validation: Drive cycle fuel consumption

The model has been fitted for driving cycle number 1 and validated in cycles 2 and 3, so that the vehicle speed are different in the cycles and the engine operating area differs in each one. Some parameters measured in the transients tests have been taken to assess the validity of the model. To validate the simulated powertrain, the energy expended by the driven wheel in the test and instantaneous engine speed during the all cycle has been compared with respect to the simulation in GT-Drive. The energy expended at the driven wheels (EWE) has been calculated according to the following expression:

$$EWE(kWh) = \int_{t_{ini}}^{t_{fin}} \frac{T_{wheel}(t) \cdot \omega_{wheel}(t)}{3.6 \cdot 10^6} \cdot dt \tag{2}$$

Where $T_{wheel}(t)$ is the instantaneous torque developed by the two driven wheels during the cycle; $\omega_{wheel}(t)$ the instantaneous wheel speed during the cycle and $3.6 \cdot 10^6$ is the conversion factor to obtain the expended energy in kWh. In Figure 4, the energy available at driven wheels in the three cycles are represented. The graph compares the energy available obtained by the simulation and the experimental test.

Also in Figures 5 the engine speed obtained from the experimental test and the engine speed obtained from the simulation are compared.

To validate the simulated engine model, the accumulated fuel consumption of the engine during the cycles have been taken as a reference.

Figure 6 compares the accumulated fuel consumption measured experimentally and the fuel consumption obtained by simulation.

As shown, there are slight differences between the experimental result and the result obtained from the simulation. However, the trend is parallel. Depending on the engine operating points the results are more accurate, since the map interpolation can introduce errors in the simulation.

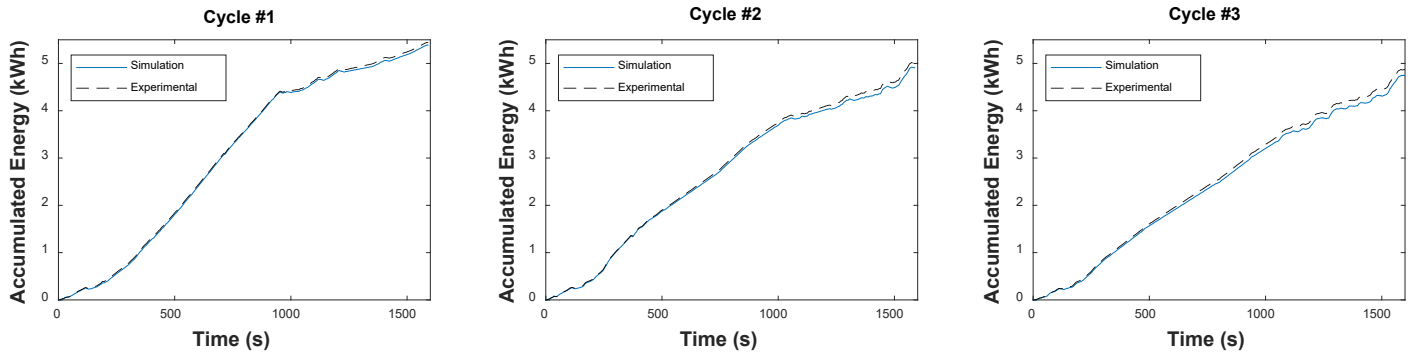

Figure 4: Expended energy in the driven wheel during driving cycles

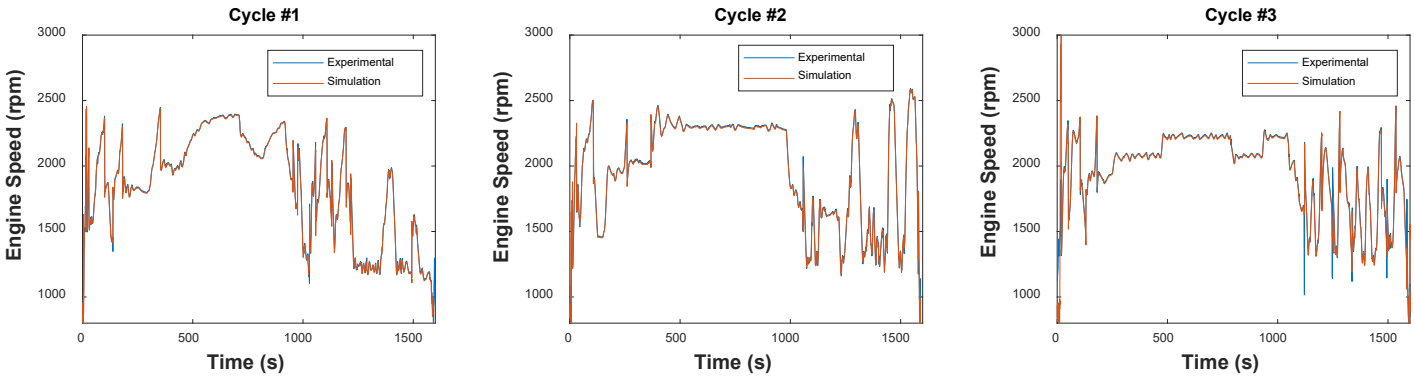

Figure 5: Engine speed during driving cycles

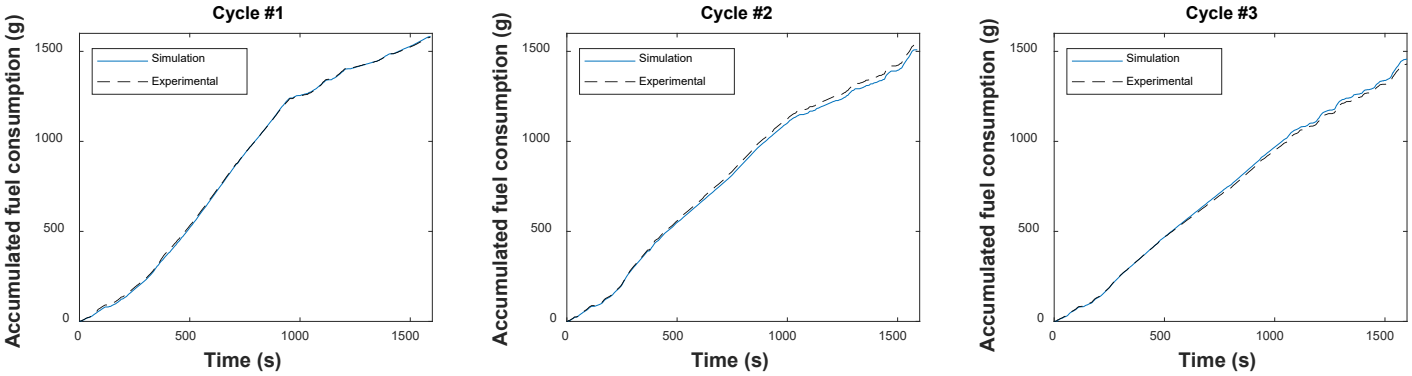

Figure 6: Accumulated fuel consumption during driving cycles.

As a summary, in table 2 shows the percentage error obtained between the experimental results and the results obtained by the simulation. This comparison shows the difference between the accumulated fuel consumption values at the end of the cycle and the total energy expended at the driven wheels at the end of the cycle.

The differences are small between the measured and the simulated cycles thus, it can be concluded that the model performs well in the driving cycles studied. Hence, it is interesting for studying variables that cannot be obtained experimentally during a driving cycle, such as: the bivariate histogram which allows to determine the operating area of the engine during the cycles. In Figure 7, the different bivariate histograms for the three driving cycles are represented. These histograms are useful in order to justify the engine performance in terms of fuel consumption, mechanical losses and engine efficiency.

In this way, the different fuel consumption of each cycle can be justified. Before that, engine consumption map and specific fuel consumption map are shown in Figure 8 derived from previous work [25].

As shows Figure 7, cycle number 2 and cycle number 3 have very similar operating area. Thus, during both cycles the average specific fuel consumption are quite similar. However, the total fuel consumed are different. As the powertrain

Table 2: Experimental vs. simulation results

		Fuel consumption (g)	Expended wheel energy (kWh)
	Experimental	1578.26	5.44
Cycle N°1	Simulation	1583.02	5.39
	Difference (%)	0.30	-0.96
	Experimental	1534.34	5.01
Cycle N°2	Simulation	1509.39	4.91
	Difference (%)	-1.62	-2.02
	Experimental	1429.70	4.87
Cycle N°3	Simulation	1457.43	4.74
	Difference (%)	1.94	-2.52

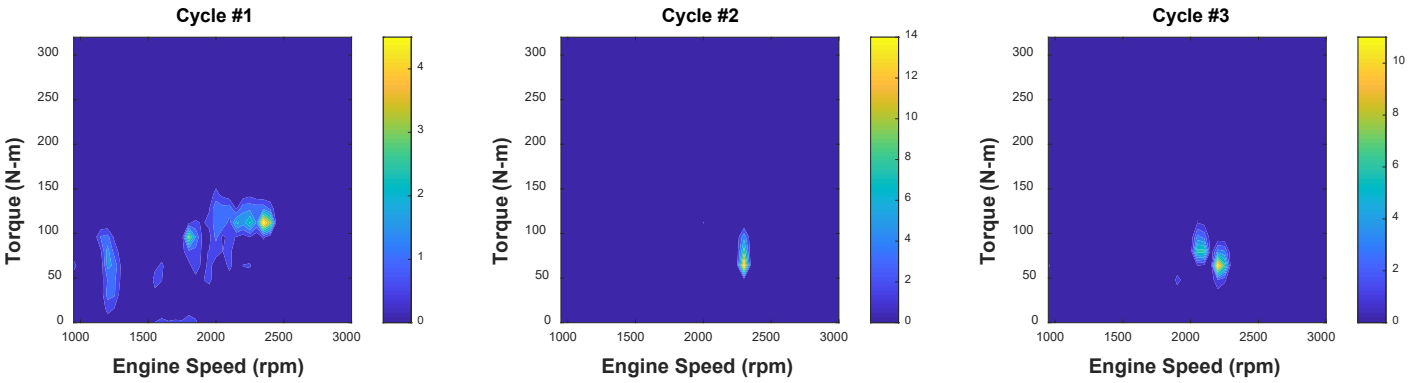

Figure 7: Time distribution in percentage during driving cycles studied

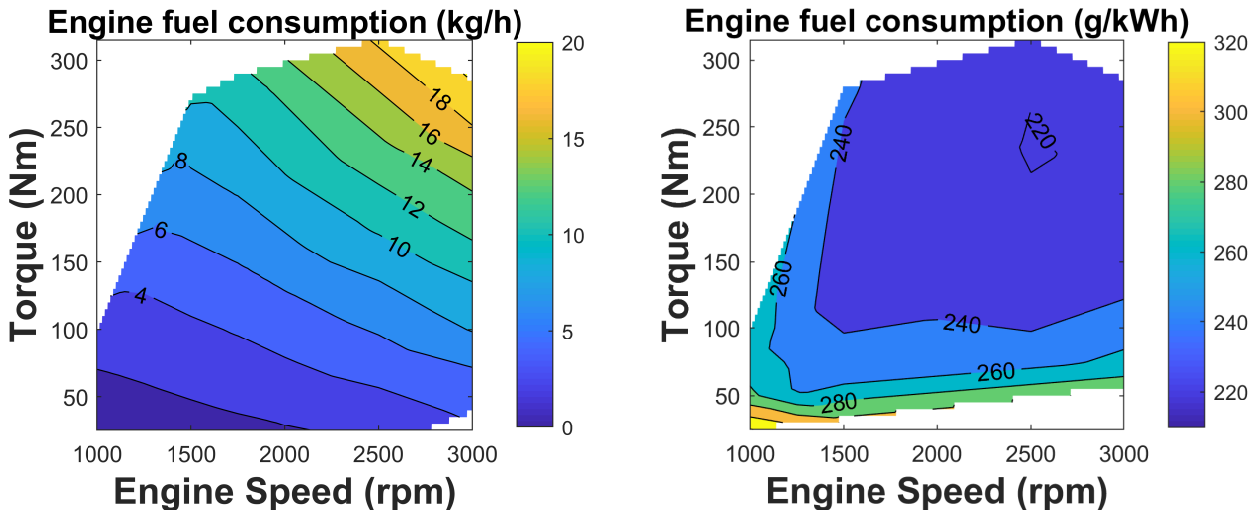

Figure 8: Left: Engine fuel consumption (kg/h). Right: Engine specific fuel consumption (g/kWh)

efficiency is the same for both cycles, higher expended energy in driven wheels, higher fuel consumption in the cycle for that reason the fuel consumption in cycle 3 is 7% higher than in cycle 2. The same analysis would be make in order to explain the mechanical losses in the engine and its distribution during the driving cycles.

4.2. Mechanical losses and its distribution during driving cycles

This section shows the calculation of the energy dissipated by engine mechanical losses during driving cycles. As demonstrated, the fitted model performs in a similar way to the engine and vehicle performance during experimental testing. Since in driving cycles the energy released in engine mechanical losses cannot be directly measured, it has been assumed that the mechanical losses calculated in the simulation (obtained from experimental map) is those that occur in the cycles tested. As demonstrated in [30], using steady-state friction engine maps in order to estimate the friction losses in a transient cycle is a good general agreement. That methodology is more accurated if the engine temperature

at cycle stars is warm conditions. In cold starting, thermal dynamic effect in engine friction are more significative due to the exponential increase of the viscosity with the temperature and the model accuracy decrease. In this work, the mechanical losses maps introduced into the model were measured under warm conditions and fixed engine oil temperature. During the driving cycle measured, the engine starting was in warm conditions, but the engine temperature differs 10 °C approximately during the test, and therefore, the friction dynamic effects could appear. Consequently, the friction losses distribution variate. However, to justify the phenomenon of non-dependence on temperature in this methodology several points of the stationary map of the engine have been assessed under two conditions:

- The distribution of mechanical losses for the experimental measured oil temperature, in the stationary tests has been calculated
- The oil temperature has been decreased 10 °C from the experimental temperature measured for each point, and the friction losses distribution has been simulated under this new temperature condition.

Figure 9 shows that the mechanical losses distribution does not change a lot according to the temperature variation in the cycles when the engine stars in warm conditions, so, the effect of the reduced temperature variations can be neglected in this work. In the carried out driving cycles test, the initial engine cooling system temperature was around 90°C. Subsequently and as developed in [25], individual maps of each pair of engine friction elements, including auxiliary losses, are used. These maps have been introduced into the software to obtain an estimation of frictional losses during driving cycles in terms of: Engine bearings, valvetrain, piston-ring assembly and auxiliaries. In Figure 10, the distribution of the mechanical losses in function of engine speed and load is presented.

Figure 11 shows the comparison between the energy lost by experimental friction, obtained from the interpolation of the mechanical losses engine maps in stationary conditions, and simulated energy friction losses obtained from interpolating the individual friction maps of each frictional element. Due to

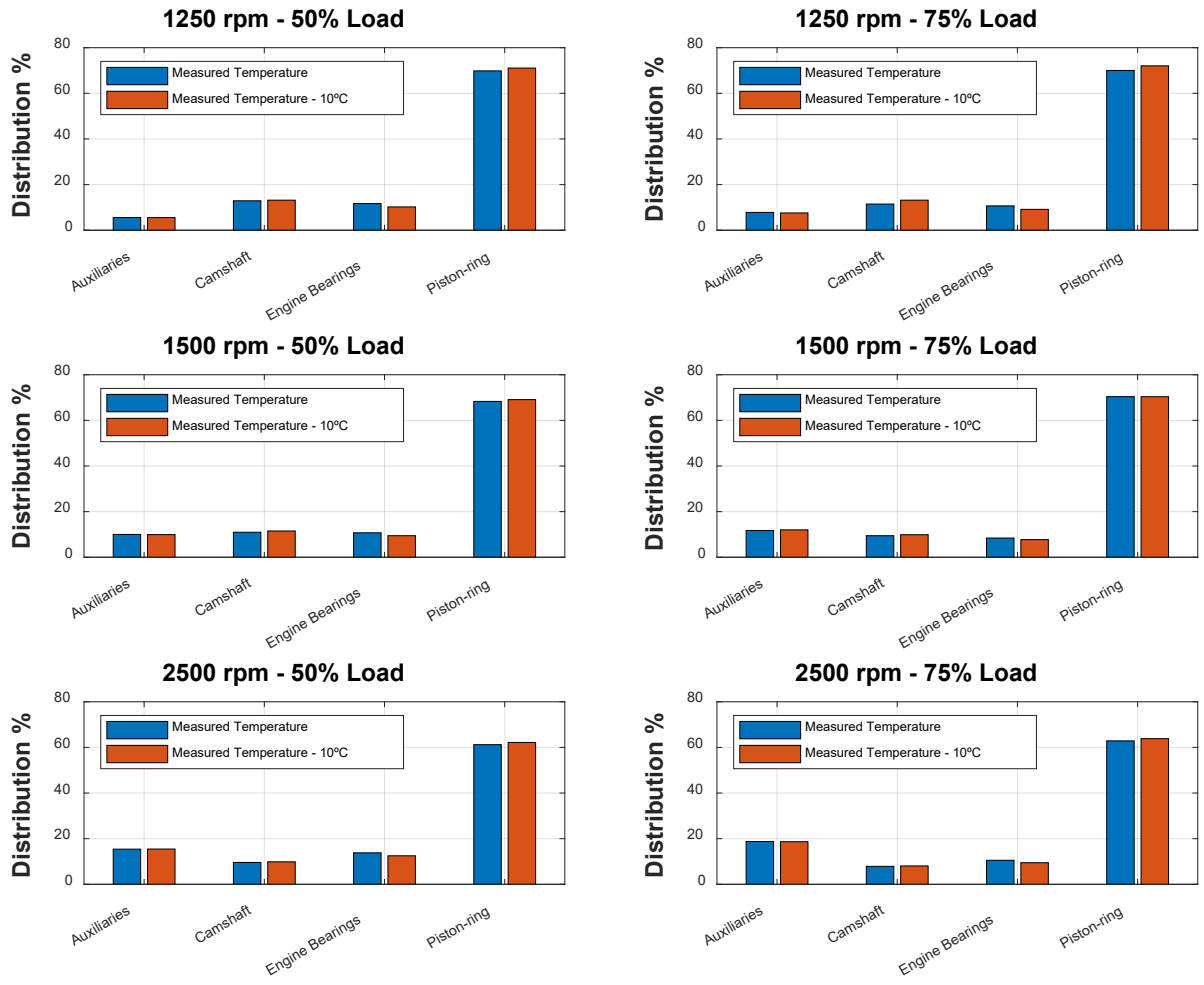

Figure 9: Variation of mechanical losses distribution with temperature

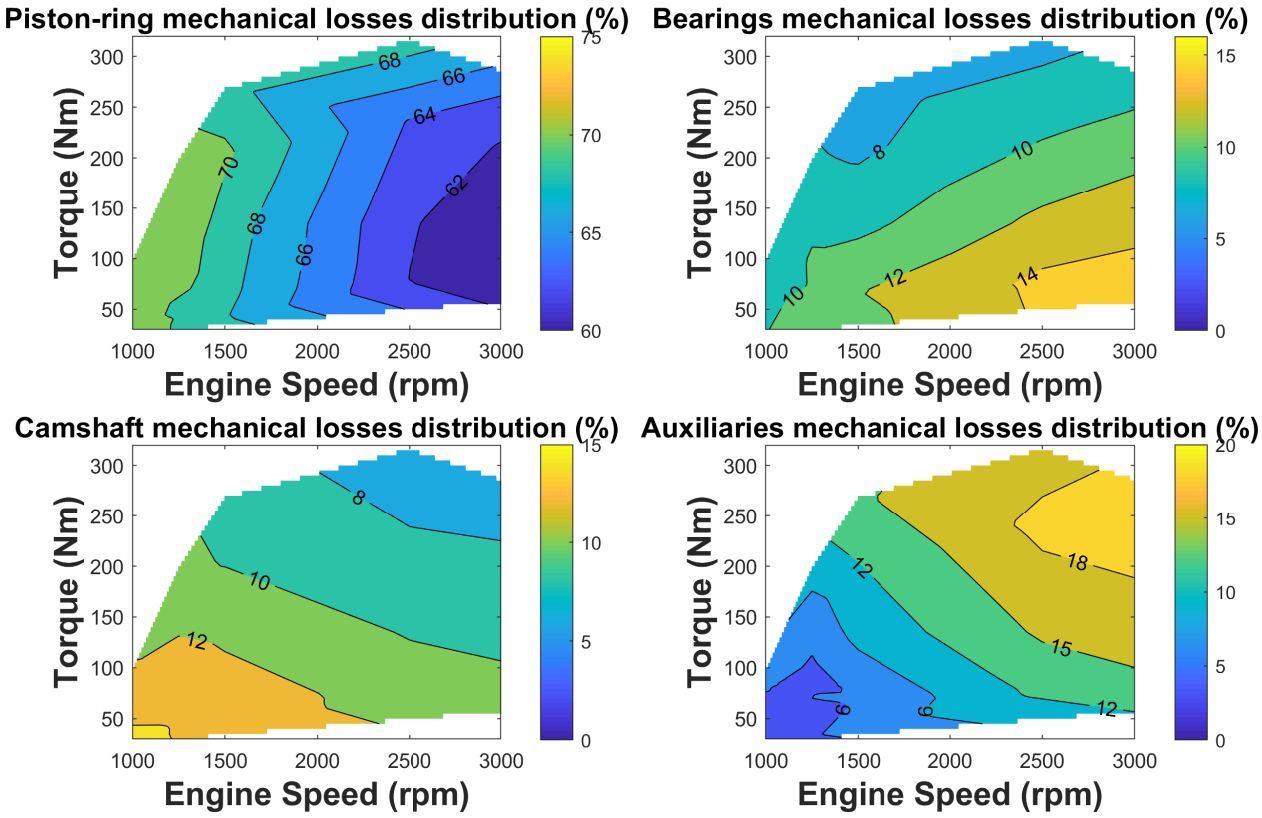

Figure 10: Friction engine maps

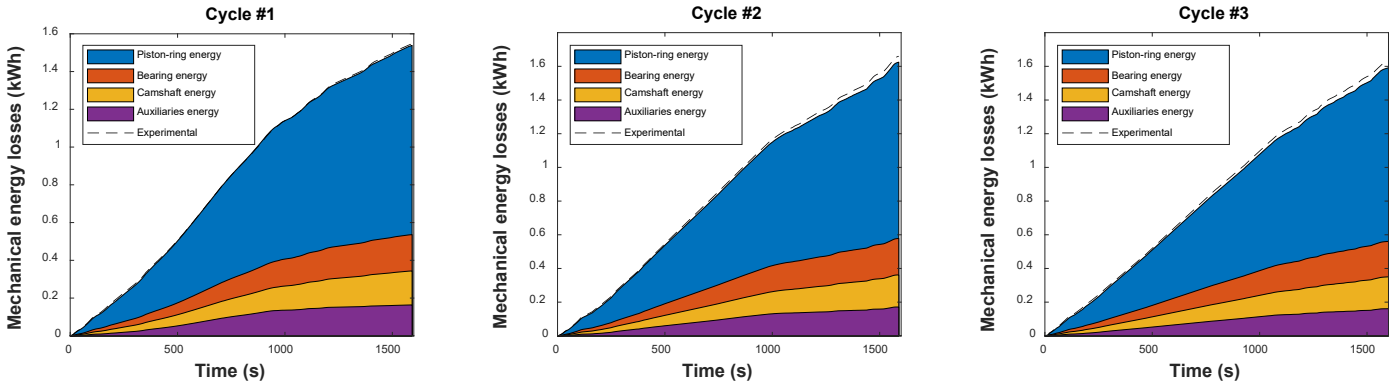

Figure 11: Mechanical losses distribution during driving cycles.

the fitting presented, it has been considered that the model reproduces the mechanical losses during the driving cycle. As can be seen, most of the lost energy corresponds to the piston-ring assembly. Their contribution is 65% of the total energy lost. Due to the operating area of the engine in the cycles number 2 and 3 are quite similar as shown before, the distribution of the mechanical losses are similar. However, the operating area of the cycle number 1 is different in comparison to others. As the engine load is quite higher in cycle 1 the distribution of the mechanical losses differ, increasing the proportion of the auxiliaries losses and decreasing the bearing and camshaft losses.

In Table 3 the obtained values and energy distribution of each frictional element during the two cycles are summarized.

The lower friction energy losses are given for cycle number 1. But the cycle N°3 needs less energy to travel the same trip during the same time. This effect results in savings in the effective power required of the engine in cycle N°3. However, the savings produced in the effective power is not proportional to that produced at the indicated power, because the engine operates at a point where the mechanical efficiency is lower for this cycle. In Figure 12 the engine mechanical losses and its efficiency are represented. The higher engine load, the higher mechanical efficiency is. As in cycle 2 as in cycle 3, the average load and

Table 3: Mechanical losses distribution during driving cycles

	Cycle N°1		Cycle N° 2		Cycle N°3	
	kWh	%	kWh	%	kWh	%
Piston-ring assembly	1.002	65.15	1.047	64.47	1.032	64.74
Engine bearings	0.192	12.48	0.216	13.30	0.211	13.24
Camshaft	0.180	11.70	0.190	11.70	0.190	11.92
Auxiliaries	0.164	10.67	0.171	10.53	0.161	10.10
Total	1.538	-	1.624	-	1.594	-

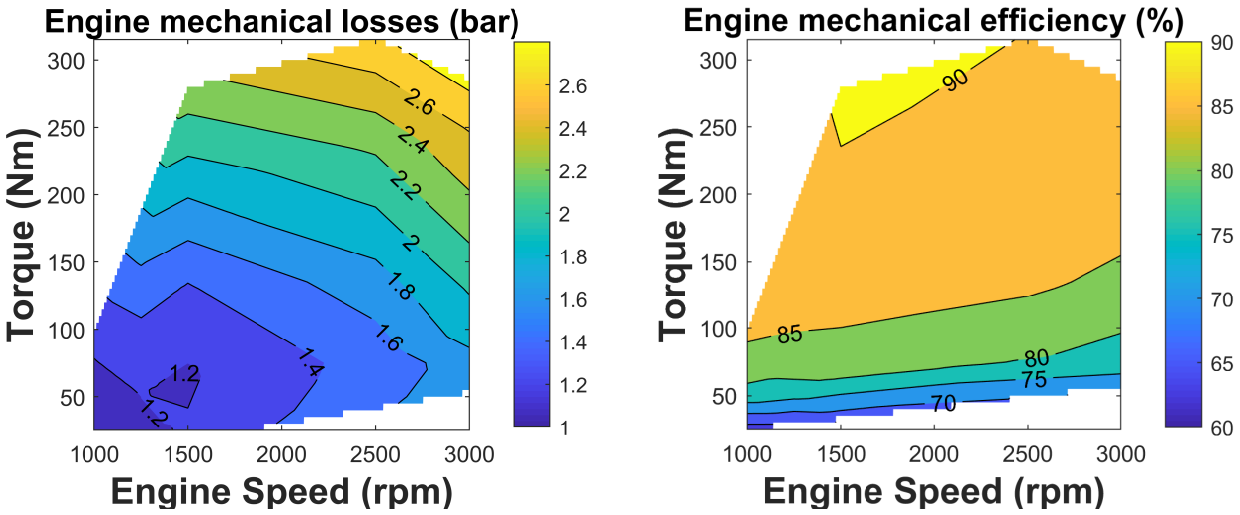

Figure 12: Left: Engine mechanical losses (bar). Right: Engine mechanical efficiency (%)

engine speed are minor than cycle 1, but, the expended energy in the wheels are higher in cycle 1 than cycle 2 and 3 and, consequently the fuel consumption is the highest in cycle number 1. However, the mechanical losses in cycle number 3 is higher than cycle number 1 in spite of the fact the fuel consumption is minimal in cycle number 3, so, it can be concluded that minimal fuel consumption it is not directly minimal engine mechanical losses.

Based on the figure 10, friction losses in the piston-ring assembly increases faster with increased engine load than with engine speed. The cycle number 1 has a higher average load than the other two cycles, so, the piston-ring distribution in that cycle are major than the other two cycles. Moreover, due to the similar operating area of the cycle number 2 and 3, the friction distribution in both cases are similar. As shown in Table 3.

However, for cycle N°3, the total percentage of energy lost by friction decreases, increasing the percentage lost by the engine bearings. For this cycle, the average engine speed is higher. Friction losses in bearings depends basically on the engine speed and therefore the bearing mechanical losses distribution is minor in comparison to the cycle 2 and 3.

5. Conclusions

In this work, a model has been developed to estimate the mechanical losses of an engine during a driving cycle using stationary maps obtained from experimental test. Moreover, parameters such as engine break torque can be estimated. That parameter are useful for a deeper engine analysis in transients cycles.

This model is valid for estimating the distribution of mechanical losses between elements with relative motion, since secondary phenomena such as oil temperature change during the cycle and friction changes due to the inertia of the elements they do not have a significant impact in the simulation results. As long as, the engine temperature in transient condition would be quite similar to the temperature in the stationary conditions when the engine maps are

obtained.

The main advantage of this model is the accuracy to predict the performance of the engine during the cycle varying parameters such as: speed profile, driving conditions... And its effect on mechanical losses to optimize fuel consumption and increase engine efficiency. However, as it has been concluded, the minimal fuel consumption it does not implies the minimal engine mechanical losses.

In addition, others parametric studies can be performed varying certain parameters such as: geometries, materials, coatings, engine lubricants used, etc. that will affect the stationary model and consequently derived results. After this studies, the stationary engine mechanical losses maps will be used later to simulate the driving cycles with an accurate prediction. This work is a useful tool to optimize the mechanical losses during a driving cycle with a relative low computational cost.

Acknowledgements

The authors would like to thank different members of the CMT-Motores Térmicos team of the Universitat Politècnica de València for their contribution to this work. The authors would also like to thank the Spanish Ministry of Science, Innovation and Universities for financing the PhD. Studies of Antonio J. Jiménez-Reyes (grant FPU18/02116).

References

[1] S. Dente, L. Tavasszy, Policy oriented emission factors for road freight transport, Transportation Research Part D (2018) 33–41doi:https://doi.org/10.1016/j.trd.2017.03.021.

[2] A. Demirbas, Progress and recent trends in biofuels, Progress in Energy and Combustion Science (2007) 1–18doi:https://doi.org/10.1016/j.pecs.2006.06.001.

[3] J. K. Mwangi, W. Lee, Y. Chang, C. Chen, L. Wang, An overview: Energy saving and pollution reduction by using green fuel blends in diesel engines, Applied Energy (2015) 214–236doi:https://doi.org/10.1016/j.apenergy.2015.08.084.

[4] K. Holmberg, A. Erdemir, The impact of tribology on energy use and CO_2 emission globally and in combustion engine and electric cars, Tribology International (2019) 389–396doi:10.1016/j.triboint.2019.03.024.

[5] A. Omari, S. Pischinger, O. P. Bhardwaj, B. Holderbaum, J. Nuottimäki, M. Honkanen, Improving engine efficiency and emission reduction potential of HVO by fuel-specific engine calibration in modern passenger car diesel applications, SAE Int. J. Fuels Lubr (2017) 10doi:10.4271/2017-01-2295.

[6] EC, Regulation no 443/2009, Setting emission performance standards for new passenger cars as part of the community's integrated approach to reduce CO_2 emissions from light-duty vehicles, Tech. rep. (2009).

[7] F. Bozza, V. D. Bellis, T. Luigi, EGR systems employment to reduce the fuel consumption of a downsized turbocharged engine at high-load operations, in: 69th Conference of the Italian Thermal Engineering Association, 2014.

[8] M. Wirth, H. Schulte, Downsizing and stratified operation - an attractive combination based on a spray-guided combustion system, in: International Conference on Automotive Technologies, 2006.

[9] J. Benajes, J. Martín, A. García, D. Villalta, A. Warey, Swirl ratio and post injection strategies to improve late cycle diffusion combustion in a light-duty diesel engine, Applied Thermal Engineering (2017) 365–376doi:10.1016/j.applthermaleng.2017.05.101.

[10] P. Olmeda, J. Martín, R. Novella, D. Blanco-Cavera, Assessing the optimum combustion under constrained conditions, International Journal of Engine Research (2018) 1–12doi:10.1016/j.applthermaleng.2017.05.101.

[11] W. Koszela, P. Pawlus, R. Reizer, T. Liskiewicz, The combined effect of surface texturing and DLC coating on the functional properties of internal combustion engines, Tribology International (2018) 470–477doi:10.1016/j.triboint.2018.06.034.

[12] R. S. Bajwa, I. Tudela, R. Verbickas, I. Palamarciuc, Y. Zhang, Friction and wear performance of sn-based coatings under hydrodynamic, mixed and boundary lubrication, Tribology Internationaldoi:,https://doi.org/10.1016/j.triboint.2019.03.053.

[13] M. Kocsis, P. Morgan, A. Michlberger, E.Delbridge, Optimizing engine oils for fuel economy with advanced test methods, SAE Int. J. Fuels Lubr (2017) 10doi:https://doi.org/10.4271/2017-01-2348.

[14] K. Holmberg, A. Erdemir, Influence of tribology on global energy consumption, costs and emissions, Friction (2017) 263–284doi:https://doi.org/10.1007/s40544-017-0183-5.

[15] H. Hongwen, G. Jinquan, P. Jiankun, T. Huachun, S. Chao, Real-time global driving cycle construction and the application to economy driving

pro system in plug-in hybrid electric vehicles, Energy (2018) 95–107doi:https://doi.org/10.1016/j.energy.2018.03.061.

[16] K. Sentoff, L. Aultman-Hall, B. Holmén, Implications of driving style and road grade for accurate vehicle activity data and emissions estimates, Transportation Research Part D (2015) 175–188doi:https://doi.org/10.1016/j.trd.2014.11.021.

[17] M. Faria, G. Duarte, R. Varella, T. Farias, P. Baptista, How do road grade, road type and driving aggressiveness impact vehicle fuel consumption? assessing potential fuel savings in Lisbon, Portugal, Transportation Research Part D (2019) 148–161doi:https://doi.org/10.1016/j.trd.2019.04.016.

[18] C. Oglieve, M. Mohammadpour, H. Rahnejat, Optimisation of the vehicle transmission and the gear-shifting strategy for the minimum fuel consumption and the minimum nitrogen oxide emissions, Proc IMechE Part D: J Automobile Engineering (2017) 883–899doi:https://doi.org/10.1177/0954407017702985.

[19] M. Montazeri-Gh, M. Naghizadeh, Development of car drive cycle for simulation of emissions and fuel economy, in: SCS Europe BVBA, 2003.

[20] S. Lee, C.Fulper, J.McDonald, M.Olechiw, Real-world emission modeling and validations using PEMS and GPS vehicle data, Sae Technical Paper Series 1 (2019-01-0757) (2016) 1–16. doi:https://doi.org/10.4271/2019-01-0757.

[21] B. Tormos, L. Ramírez, J. Johansson, M. Björling, R. Larsson, Fuel consumption and friction benefits of low viscosity engine oils for heavy duty applications, Tribology International (2017) 23–34doi:https://doi.org/10.1016/j.triboint.2017.02.007.

[22] V. Macián, B. Tormos, S. Ruiz, G. Miró, Low viscosity engine oils: Study of wear effects and oil key parameters in a heavy duty engine fleet test,

Tribology International (2016) 240–248doi:https://doi.org/10.1016/j.triboint.2015.08.028.

[23] V. Macián, B. Tormos, S. Ruiz, L. Ramírez, Potential of low viscosity oils to reduce CO_2 emissions and fuel consumption of urban buses fleets, Transportation Research Part D: Transport and Environment (2015) 76–88doi:https://doi.org/10.1016/j.trd.2015.06.006.

[24] V. Macián, B. Tormos, V. Bermúdez, L. Ramírez, Assessment of the effect of low viscosity oils usage on a light duty diesel engine fuel consumption in stationary and transient conditions, Tribology International (2014) 132–139doi:https://doi.org/10.1016/j.triboint.2014.06.003.

[25] B. Tormos, J. Martin, D. Blanco-Cavero, A. Jimenez-Reyes, One-dimensional modeling of mechanical and friction losses distribution in a 4-stroke internal combustion engine, Journal of Tribology (2019) 1–34doi:10.1115/1.4044856.

[26] F. Payri, J. M. Lujan, J. Martin, A. Abbad, Digital signal processing of in-cylinder pressure for combustion diagnosis of internal combustion engines, Mech Syst Signal Process 6 (2010) 1767–1784. doi:10.1016/j.ymssp.2009.12.011.

[27] N. Fraser, H. Blaxill, G. Lumsden, M. Basset, Challenges for increased efficiency through gasoline engine downsizing, SAE International Journal of Engines 2 (1) (2009) 991–1008. doi:https://doi.org/10.4271/2009-01-1053.

[28] B. Ciuffo, G.Fontaras, Model and scientific tools for regulatory purposes: The case of CO_2 emissions from light duty vehicles in europe, Energy Policy 109 (2016) 76–81. doi:https://doi.org/10.1016/j.enpol.2017.06.057.

[29] J. Benajes, A. García, J. Monsalve-Serrano, R. Lago, Fuel consumption and engine-out emissions estimations of a light-duty engine running in dual-

mode RCCI/CDC with different fuels and driving cycles, Energy 157 (2018) 19–30. doi:https://doi.org/10.1016/j.energy.2018.05.144.

[30] T. Funk, H. Ehnis, R. Kuenzel, M. Bargende, Validity of a steady-state friction model for determining CO_2 emissions in transient driving cycles, SAE Technical Paper (2019-24-0054).